

Research Article

Urban Expansion Trends, Prediction and Its Impact on Agricultural Lands in Erbil Using GIS and Remote Sensing

Barzan Sabah Aziz ^{1,*} , Ali Volkan Bilgili ¹ , Mehmet Ali Çullu ¹ , Fred Barış Ernst ² , Soran Omar Ahmed ¹ 

¹ Department of Soil Science and Plant Nutrition, Faculty of Agriculture, Harran University, Şanlıurfa, 63050, Turkey

² Department of Geomatics Engineering, Faculty of Engineering, Harran University, Şanlıurfa, 63050, Turkey

*Corresponding Author: Barzan Sabah Aziz, E-mail: barzanengn@gmail.com

Article Info	Abstract
Article History	The surrounding agricultural lands in the city have been decreasing daily due to the expansion of urbanisation above it and the increase in the urbanisation rate in the study area, as the population growth exerted increasing pressures on the city. Furthermore, the increase in population increases the demand for land for housing and other human services, impacting agricultural lands. In addition, the lack of proper planning in the city contributes to expanding urbanisation at the expense of agricultural land. This study aims to study the urban expansion in the direction of agricultural lands in Erbil from the year 2000 until 2020, reveal the reasons for the urban expansion in the city, and put an end to the trespassers on the lands. It has a negative impact on the lack of agricultural areas and the encroachment of urbanisation on it. Landsat TM 5 and Landsat 8 OLI will be used to identify and develop urban growth and its impacts on agriculture and some Remote sensing Data and GIS from 2000 to 2020 with 10 years difference to find the changes in these years and also provide a predicted map for Erbil governorate. The study recommended the necessity of preparing a strategic plan for the use of agricultural lands that regulates the urban development process of the population centres and achieves the appropriate and sustainable use of agricultural lands and their preservation—encouraging the investment of lands and cultivation of crops to meet the population's need for vegetables and other crops. The findings of this study will help decision-makers develop future urbanisation policies, and it is worthwhile to investigate them further. The prediction model will demonstrate whether built-up areas will continue to grow or not and whether the average agricultural areas will continue to shrink based on regression analysis. Planning effective urban environmental management can benefit from this type of forecast of the LULC picture in the future.
Received Jul 20, 2022	
Revised Aug 1, 2022	
Accepted Aug 10, 2022	
Keywords	
Change Detection	
Change prediction	
LCM	
CA Markov	
GIS	
Remote Sensing	



Copyright: © 2022 Barzan S. Aziz, Ali Volkan Bilgili, Mehmet Ali Çullu, Fred Barış Ernst and Soran O. Ahmed:

This article is an open-access article distributed under the terms and conditions of the Creative Commons Attribution (CC BY 4.0) license.

1. Introduction

According to certain definitions, urbanisation is a cross-sectoral process that affects all facets of human society and the economy [1]. The primary resource of human civilisation is land, fixed by nature and does not rise with the population. More land is required because of growing urbanisation and population.

Agricultural land is often reduced due to land use for residential, industrial, municipal, and other reasons, lowering agricultural yield [2].

In the previous two decades, urban growth has increased significantly and has continued to rise. Agricultural and natural regions might be destroyed due to rapid urban growth. Although many cities were built without considering this, controlling this growth is crucial. Cities with rising population densities prioritise the development of rural and natural regions. The study assumed a set of hypotheses: Agricultural land is decreasing in the study area, and urban encroachment affects agricultural areas. Urban population growth outpaces rural decline due to population migrations [3]. The effect will be a transformation in the types of agricultural land to barren land or urbanised land since this lowers worker productivity in agricultural regions and leads these areas to stay dormant.

Reasons for choosing the subject and choice of this topic for these reasons, the primary objective of this study is the desire of the researcher to apply Modern techniques in the study of agricultural resource management and identify agricultural areas affected by urbanisation in the study area. The Landsat satellite photos from 2000, 2010, and 2020 are being used as a supplementary purpose to forecast and assess my research region's current and future expansion. Land Change Modeler (LCM) and CA Markov IDRISI software will be used to analyse the land use and land cover changes between various classes and predict the future scenario during the research period.

Satellite imagery and remote sensing are the best techniques to detect and predict this change. Recent technologies like the Geographic Information System (GIS) and Remote Sensing (RS) in presenting and creating the decision support tools of the spatial modelling approach have aided in the expansion and forecasting of urban areas. Our day is characterised by urbanisation. This century has experienced more change than any other in human history because of all the many factors at play. Urban studies are covered in many different contexts in a sizable and expanding body of literature. Previous research has employed two main methods to quantify the loss of agricultural land due to urbanisation. First, information on loss was obtained using socioeconomic statistics data depending on administrative units [4].

There is little knowledge of the connections between the two main developments that are happening on China's agricultural lands: the urbanisation of these areas and the intensification of agricultural land use.

An expansion in urban development and a decrease in agricultural land are both indicated by urban land expansion. It is projected that a lack of land would result in more intense agricultural land usage [5].

Rapid urbanisation causes fierce rivalry, a rise in the demand for built-up areas, and the need to conserve agricultural land, forests, and arable land. As a result, recognising the ongoing expansion of land resources has grown to be quite difficult [6].

Over the last several decades, European agricultural land usage has significantly transformed. The observed changes showed changes in the amount of agricultural land, the intensity of land management, and agricultural land use activity. Significant land use change trends are related to the international growth of agricultural markets, the shift from a rural to an urban society, and the transformation from socialism to post-socialism in central and Eastern Europe [7].

Land use and cover change is the most significant anthropogenic driver of environmental change at all geographical and temporal dimensions. Climate change, biodiversity loss, and water, soil, and air pollution are among modern human populations' biggest environmental worries. Consequently, it has become a top concern for academics and policymakers worldwide to monitor and mitigate the harmful effects of LULC while maintaining the production of key resources. It has evolved into the focal centre of study in natural resource management. A region's land use and cover pattern result from how people have used social and economic elements throughout time and geography. Land use is how people use the land, whereas land cover is the actual physical and biological cover of the land. Knowledge of land cover and land use change is crucial for many planning and management tasks. In combination with geographic information systems (GIS), satellite remote sensing has been widely used and acknowledged as a potent and useful tool for identifying changes in land use and land cover. Satellite remote sensing offers reasonably priced multi-spectral and multi-temporal data. It transforms them into information useful for comprehending and tracking patterns and processes of land development and accumulating land use and land cover data sets over time. The flexible environment offered by GIS technology makes it possible to store, analyse, and display the digital data required for database creation and change detection. Studies on change detection using remote sensing and GIS have mostly concentrated on determining how much, where, and what kind of land use and land cover change has occurred.

Modern civilisations face enormous hurdles due to issues with urbanisation and the concentration of people in major metropolitan regions. Urban expansion is fueled by economic growth and takes the form of building companies, homes, highways, recreation centres, etc. Metropolitan areas struggle with the expanding effects of urban sprawl, including a loss of natural flora, animal habitats, and agricultural land. Residential and commercial construction is replacing undeveloped land at an unprecedented rate. In comparison to other places, the coastal areas are said to have the highest levels of human intervention with the landscape, home to almost 60% of the world's population. A rise in resource consumption, an increase in human population, and the growth of metropolitan areas are some environmental variables influencing the environment and eventually producing rapid changes in the terrain [8].

2. Material and Methods

2.1. Study area

The Erbil government is located in northern Iraq, 350 kilometres from Baghdad. Suleimanya is situated southeast of Erbil, Dohuk and Mosul are situated west of Erbil, while Kirkuk is situated east of Erbil. Along the north and northeast of Erbil, there is an international boundary between Turkey and Iran, which is located between $36^{\circ} 11' 28''$ N and $44^{\circ} 0' 33''$ E. A Mediterranean climate characterises Erbil, with long, sweltering summers and moderate winters. Little precipitation between June and September makes the summer months particularly dry. Typically, January is the wettest month of the winter, which is also the most humid. Although a wide area of land surrounds Erbil, the lands in the North part of Erbil city were very fertile and suitable for farming, like the Harir and Sidakan area, which could be used for different kinds of farming, but the Southern part of Erbil city only use for some kinds of crops such as wheat and barley, due to its soil which contain a high amount of calcium carbonate and it was a negative effect of soil productivity (Figure 1).

2.2. Data Types and Sources

For the current research, Erbil's multispectral, multitemporal LANDSAT satellite data were collected for the three years 2000, 2010, and 2020. All the LANDSAT images have been taken from the United States

Geologic Survey (USGS). The 2000 and 2010 images are thematic mapper images, and 2020 is Landsat 8 OLI. They have a resolution of 30 meters.

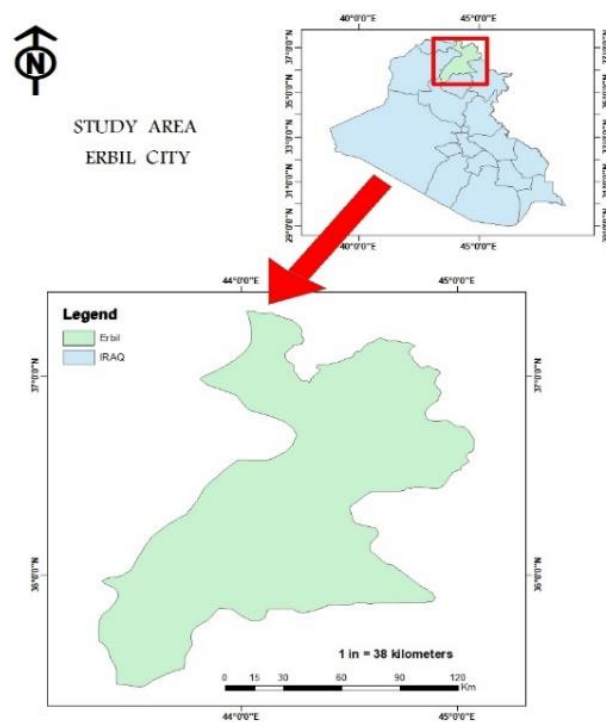


Figure 1. Shown Study Area of Erbil

We projected all satellite photos using the Universal Transverse Mercator (UTM) method. UTM projection system projected all the data used in the study, Zone 38 WGS4 1986 North for Erbil, the Landsat satellite of 30m spatial resolution for each study area is satisfactory to present human development; other categories of land-use from other kinds of land-cover change are identified by the spectral range of the tool. The secondary data collected from the Directorate of Agriculture supplied the data on the Internet. The Governorate and Municipality will have maps such as the municipal boundaries, geographical, ward, and master plan maps. Table 1 lists the data obtained, their production date, resolution, and source.

Table 1. Details of the Landsat image data were used to analyse the research area's land use and land cover (LULC).

Satellite Sensor	Path/Row	AcquisitionDate	User Bands	Resolution Spatial	Year
Landsat 7 ETM+	169/35, 169/34	June 2000	1–5, 7	30 m	2000
Landsat 7 ETM+	169/35, 169/34	June 2010	1–5, 7	30 m, 15 m	2010
Landsat 8 OIL	169/35, 169/34	June 2020	1–5, 7	30 m, 15 m	2020

2.3. Pre-Processing and Image Classification

2.3.1. Pre-Processing

Landsat photos typically cover enormous areas in hectares (ha), but this study and each study area required smaller hectares, thus, the Landsat images were cropped to the bounding box that encloses the study region. In addition, Landsat pictures were in the GeoTIFF* format. A TIFF (picture) file can contain georeferencing data thanks to the public domain metadata standard called GeoTIFF (GeoTIFF, n.d.). Furthermore, images have been exported to the ENVI and ERDAS IMAGINE** formats for various programs, particularly IDRISI. Finally, the vector data for Erbil, obtained from Landsat Zone 38 WGS4 1986 North and has a 30 m spatial resolution for each research region, was clipped to the study area.

*A TIFF (picture) file can contain georeferencing data thanks to the public domain metadata standard called GeoTIFF (GeoTIFF, n.d.).

**The remote sensing program ERDAS IMAGINE

2.3.2. Image Classification

Obtaining the land use/cover classifications from remote sensing sources using classification techniques was the first investigation stage in figure 2, the categorisation workflow.

2.3.3. Using Land Classification of Land Cover

Satellite, the production of LULC maps involves image classification techniques. LULC maps with a temporal component were produced using image classification [9]. Three distinct LULC patterns (2000, 2010, and 2020) were created. For the years 2000 through 2010, Landsat 7 ETM between $36^{\circ} 11' 28''$ N and $44^{\circ} 0' 33''$ E, with row/path 169/35 and 169/34, and Landsat 8 ("OLI TIRS") with row/path 169/35 and 169/34 Erbil, Iraq. A map of land usage and land cover was created with a ground resolution of 30 meters. With histogram equalisation, atmosphere and haze correction, and ENVI 5.3, Landsat pictures have been modified to increase their visual quality. The Landsat image was classified using supervised classification methods. Reference training sites for each LULC class were used to create training signatures. False colour composite Landsat pictures were shown in the image viewer. In ENVI 5.3, signature polygons were made using the signature editor's tools from the categorisation menu. Areas of Interest (AOI) that resembled comparable LULC-type characteristics were drawn in the picture viewer.

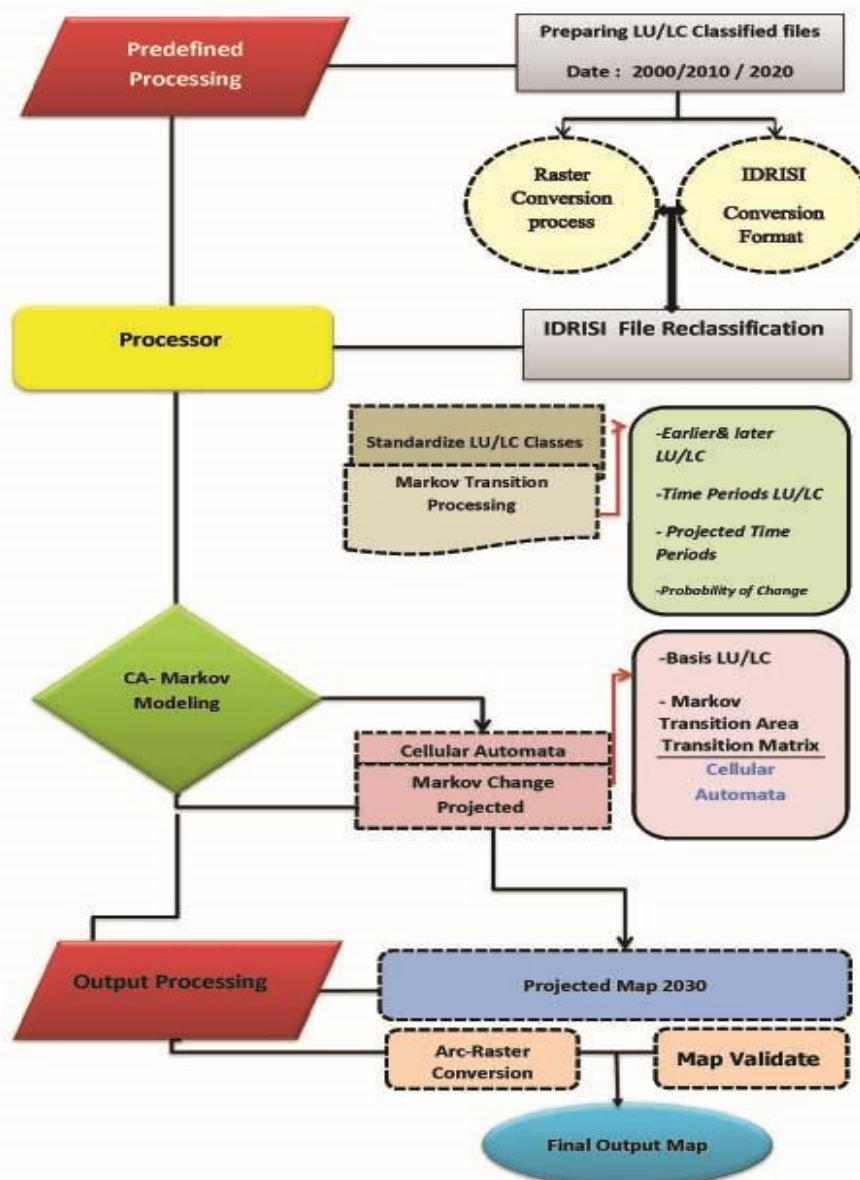


Figure 2. Workflow of clarifying steps of study methodology Classification

These AOI were used to establish signatures that represented various LULC types. Before combining them into a single hallmark class, many training locations for each type of LULC were created, each with a unique set of features. The separation of each class of signatures was verified during supervised classification. The supervised classification method employed was the maximum likelihood method. The kind of terrain and its cover were discovered during the classifying procedure. LULC was divided into three categories: 1) built-up, 2) bare, 3) agriculture, 4) grass, and 5) Forest. Five distinct LULC are listed in Table 2, each description.

Table 2. The main categories of land cover and their explanations.

Agricultural Land	Comprises irrigated regions, rural outposts, commercial farms, and areas utilised for perennial and annual crops (sesame cultivations and sugarcane plantations).
Forest Land	Areas with many trees (deciduous forests, evergreen forests, mixed forests).
Range Land	Includes places with sparse woods, plants, and shrubs and those with little trees. Compared to woods, these places are less dense.
Grass Land	Grazing is often done in grassy areas, which are there for a few months of the year.
Urban Area	Business districts, urban and rural communities, and industrial zones.
Water Body	Regions where rivers, streams, and reservoirs are present.

The ERDAS Imagine 2014, and ArcGIS 10.3 software was used to achieve picture classification using a multi-temporal method and for mapping reasons. Based on the composite photos and Google Earth images, as many training samples as feasible were chosen for each LULC from the full image. The training data were utilised for categorisation, verification, and validation of the categorised pictures.

2.3.4. Accuracy Assessment

The accuracy evaluation determines how accurately the corresponding categorised image represents the ground reality. The classification results' accuracy must be evaluated since land use maps produced using image classification typically contain some mistakes. Determine the level of confidence in the findings and the subsequent change detection by evaluating the classification accuracy. The categorised map was compared with real-world data to determine its correctness. The reference points were gathered for 2000 and 2010 using Google Earth, the original Landsat pictures, interviews, group discussions, earlier reports, and maps. In addition, Google Earth, in-person observations, authentic Landsat photos, interviews, and group discussions on arbitrary reference sites in various LULC kinds were recorded from the field survey carried out by GPS for the 2020 image. An error/confusion matrix is the most popular and efficient way to assess the precision of the categorised picture from remotely sensed photography. The confusion matrix offers kappa data, producer accuracy, user accuracy, and total accuracy. Equation (1) was used to determine the Kappa coefficient. The authors assert that a kappa coefficient value less than 0.4 indicates a

lack of agreement, one between 0.4 and 0.8 indicates a degree of agreement, and one larger than 0.8 indicates a substantial agreement.

$$K = \frac{N \sum_{i=1}^r X_{ii} - \sum_{i=1}^r (X_{i+}) * (X_{+i})}{N^2 - \sum_{i=1}^r (X_{i+}) * (X_{+i})} \quad (1)$$

$$K = \frac{(Total * sum\ of\ correct) - sum\ of\ all\ the\ (row\ total * column\ total)}{Total\ squared - sum\ of\ all\ the\ (row\ total * column\ total)} \quad (2)$$

where r —rows number in the matrix, X_{ii} - number of observations in row i and column i (the diagonal elements), X_{+i} and X_{i+} - the marginal totals of row i and column i , respectively, and N —observations number.

2.3.5. Change Detection Analysing using LCM

Detecting changes in an object or phenomenon by monitoring it at various intervals is the change detection method [10]. Numerous reasons may have contributed to the land change; to study these variables, we must first assess the changes. Transitions from one category to another may be seen using the change detection approach, which can aid in understanding how the categories interact. There are several methods for detecting changes. Cross tabulation, area computation, reclassification, and overlay procedures were employed for this study. A cross-tabulation statistical method displays the combined distribution of two or more variables. Reclassification is the simple process of assigning a single picture to new categories. Overlay simply refers to mixing data from many layers. These techniques determined each category's gain and loss, net change, and contributor to change [11]. Changes in each area have been noted using this methodology.

There are gains and losses in every class, as can be shown. Some of these are true changes brought on by the incorrect categorisation of the satellite photos, while others are unreliable changes in the research region. In order to comprehend the change tendency in the research region, changes in 2020 were also explored after changes in 2000 were noted. Each class gains and losses, as seen in the picture below. The primary changes are from farmland to urban areas and back again.

2.3.6. Land Use and Land Cover Change Modeling

Numerous research on LULC change modelling have been conducted, and this research may be divided into agent-based and pattern-based models. Agent-based or actor-based models are built around the

actors who control the simulation. Pattern-based models, meanwhile, primarily rely on spatial land cover data and changes through time [12]. Pattern-based models that are most widely used include.

- Cellular Automata (CA)
- Artificial Neural Networks (ANN) and Markov Chain
- Spatial Statistics (Markov Chain)

In this study, each model's outcomes were evaluated, and the approach that produced the best simulation of the LULC map for 2030 was the combination of CA and MARKOV techniques and the combination of MLP and MARKOV approaches.

2.3.7. Model Validation

Simply put, validation compares the anticipated LULC map's accuracy to a reference map. To replicate the 2020 LULC picture, Landsat photos from 2000 and 2010 were used. A comparison between the real map and the simulated LULC picture was created. LCM was calibrated using the LULC from 2000 and 2010, and the Model was then tested using a simulation of the most recent LULC map from 2020. A cross-tabulation in a three-way comparison between the later land cover map (2010), the anticipated land cover map (2020), and the actual map is used in the LCM validation process (2020). Comparing the anticipated 2020 LULC picture to the 2020 reference image allowed us to evaluate the quality of the image statistically. The map displays regions that the Model accurately predicted as "hits," regions that the Model properly anticipated as "false alarms," and regions that the Model was unable to predict, but that saw change as "misses." The simulation technique was performed to project the 2030 map using the 2010 and 2020 categorised maps after the Model's capacity for prediction between the 2000 and 2010 time periods for 2020 had been confirmed. The alternative technique is the determination of the kappa coefficient between the anticipated map and the actual land use map. The original kappa coefficient limits its expressiveness and does not differentiate between the location and quantification errors. Calculating the cause-dependent K-indices, K_{no} (kappa for no information), $K_{location}$, $K_{standard}$, and $K_{locationStrata}$ can help solve this problem (kappa for stratum-level location). The predicted and reference map's general agreement reveals the Kappa for no information (K_{no}). Due to the accurate allocation values in each category between the simulated and reference maps, the location kappa ($K_{location}$) is employed to calculate the spatial accuracy in the entire landscape. The kappa for standard deviation is the ratio of incorrect assignments made by

chance to correct assignments (Kstandard). The spatial accuracy inside previously defined strata is measured using the kappa for stratum level location (KlocationStrata), which shows how effectively the grid cells are placed within the strata. A combination of the Kstandard, Kno, Klocation, and Klocation strata scores is considered to evaluate the total accuracy in terms of location and quantity. Other statistics, such as Agreement Quantity, Agreement Chance, Agreement Grid Cell, Disagreement Grid Cell, and Disagreement Quantity, can be used to assess how strong the agreement is between the simulated map and the base map (Table 3).

Table 3. Possible map comparative ranges and kappa value levels of agreement.

No.	Values	Strength of Agreement
1	<0	Poor
2	0.01–0.40	Slight
3	0.41–0.60	Moderate
4	0.61–0.80	Substantial
5	0.81–1.00	Almost Perfect

To comprehend the simulated Model, it is essential to understand the Disagreement Quantity and Disagreement Grid Cell components. This validation technique provides insight into how closely the projected and real LULC maps agree or disagree. The amount (changes or persistence) and allocation of the two categories maps are where there are the two biggest variations. The difference between two photographs caused by an improper combination of the total LULC category proportions is known as disagreement by amount. The difference between the two pictures due to an insufficient combination of the spatial allocations of all land cover map categories is known as the allocation disagreement.

3. Results and Discussion

3.1. Accuracy Assessment of the Classified Images

By creating confusion/error matrices for each LULC category of the classed maps from 2000, 2010, and 2020, the accuracy of the LULC change analysis was evaluated. For evaluation, kappa statistics, producer and user accuracy, and total accuracy, were employed. For the years 2000, 2010, and 2020, the overall accuracy and kappa statistics of categorised pictures indicate 99.92%, 99.89%, and 99.94%, as well as 0.93,

0.92, and 0.94% (Table 4). The most recent LULC map accuracy scores were better, which might be attributed to trying more categorisation and using satellite photos with higher spatial resolution.

Any research employing historical LULC derived from remote sensing Landsat data is required to evaluate LULC accurately. The classified map's accuracy is measured, according to the authors of LULC, by constructing an error matrix or confusion matrix, which contrasts the classified map with a reference classification map. The study's findings are in line with those of several previous research. This study's accuracy demonstrates that the outcome is within the margin of the precision allowed by the Land Change Modele and Landsat photos used.

3.2. LULC and Change Analysis using LCM

3.2.1. Supervised Classification

During the years 2000, 2010, and 2020, a supervised classification algorithm was employed to generate the LULC map of Erbil. This section displays the overall land use distribution and covers it with precision. All three imageries for the years (2000, 2010, and 2020) in Erbil were classified using satellite image technology. Each image was divided into six categories for categorisation. Table 4 lists the specifics of these classes.

Table 4. The area coverage of LULC, percent, and rate between 2000, 2010, and 2020.

LULC Types	LU/LC -year 2000		LU/LC -year 2010		LU/LC-year2020	
	Km	%	km	%	km	%
Urban land	195.00	1.31	296.80	1.45	541.22	3.67
Agriculture land	2840.18	19.11	2603.05	17.50	2525.08	16.97
Barren land	4998.62	23.52	4880.15	21.50	5530.41	37.18
Forest	1522.48	20.32	2011.10	22.25	1629.62	10.95
Grass land	4794.95	32.23	4378.69	31.50	4247.53	28.55
Water	72.64	0.48	102.73	1.18	127.94	0.86
Un-classified	5.06	0.03	5.55	0.03	5.71	0.03
Glaciers	443.76	2.98	594.62	4.59	265.18	1.78

The statistic shows a massive increase in built-up area and a decrease in agricultural lands and grasslands from 2000 to 2020. For example, in Erbil in 2000, the built-up area was 195 km² (1.31%), the agricultural land area was 2840.18km² (19.11%), the barren land area was 4998.62 km² (23.52%), the forest was 1522.48 km² (20.32%), grassland was 4794.95 km² (23.23%), and water body was 72.64 km² (0.48%). The classification results of 2010 show that the built-ups were 296.80 km² (1.45%), the agricultural land

area was 2603.05km² (17.50%), the barren land area was 4880.15 km² (21.50%), and the forest was 2011.10 km² (22.25%), grassland was 4378.69 km² (31.50%), and water body was 102.73 km² (1.18%). Whereas in 2020, the built-ups were 541.42 km² (3.67%), the agricultural land area was 2525.08km² (16.97%), the barren land area was 5530.41km² (37.18%), the forest was 1629.62 km² (10.95%), grassland was 4274.53 km² (28.55%), and water body was 127.94km² (0.86%) of all area. Table 4 provides the data details for each year. According to data, there has been a general decline in both agricultural areas and grasslands of 315.10 km², 2.11 percent, and 547.42 km², 3.6%, respectively, and the built-up areas have increased (346.22 km², 2.32%) from 2000 to 2020. Figure 3's maps, which illustrate LULC categorisation for 2000, 2010, and 2020, indicate these developments.

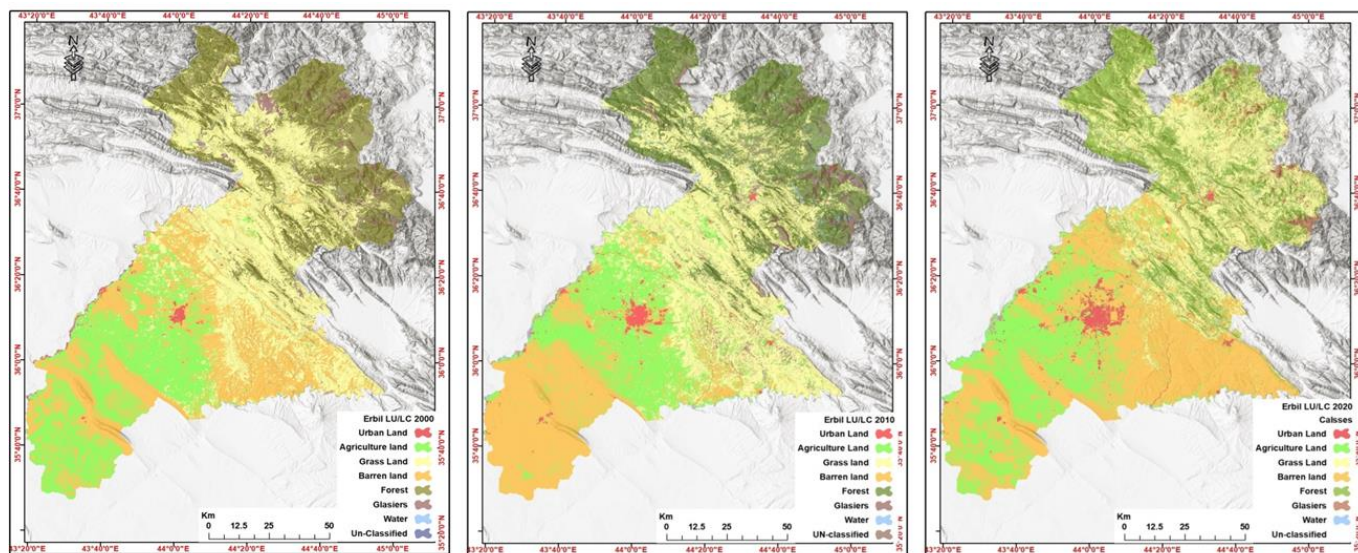


Figure 3. The LULC of the Erbil in 2000, 2010, and 2020.

3.2.2. Change analysis using LCM

The examination of gains, net changes, and losses incurred by various categories employing change analysis in LCM were how the LULC analysis changed. In addition, analysis was done to compare geographical and temporal variations between classes during 2000, 2010, and 2020. In Table 4, Figures 4 and 5, the "from-to" transformations are condensed as loss, gain, and net change of LULC. The gain of LULC for each class was calculated using the total column value and the persistence result. In contrast, the loss was calculated using the total row value and the persistence.

Table 5. The area coverage of LULC, percent, and rate of changes between 2000, 2010, and 2020.

LULC Types	LU/LC -year 2000		LU/LC -year 2010		LU/LC-year2020 Change between 2000-2020			
	Km	%	km	%	km	%	km	%
Urban land	195.00	1.31	296.80	1.45	541.22	3.67	346.22	2.33
Agriculture land	2840.18	19.11	2603.05	17.50	2525.08	16.97	-315.10	-2.12
Barren land	4998.62	23.52	4880.15	21.50	5530.41	37.18	531.79	3.58
Forest	1522.48	20.32	2011.10	22.25	1629.62	10.95	107.14	0.72
Grass land	4794.95	32.23	4378.69	31.50	4247.53	28.55	-547.42	-3.68
Water	72.64	0.48	102.73	1.18	127.94	0.86	55.30	0.37
Un-classified	5.06	0.03	5.55	0.03	5.71	0.03	0.64	0.00
Glaciers	443.76	2.98	594.62	4.59	265.18	1.78	-178.57	-1.20

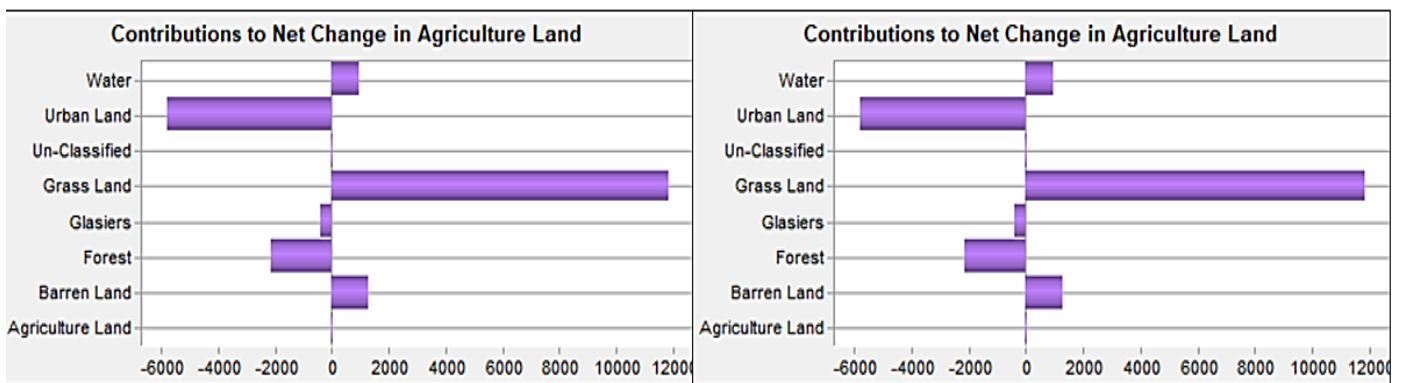


Figure 4. The land use cover class's gain and loss areas between 1990 and 2005 and 2005 and 2009

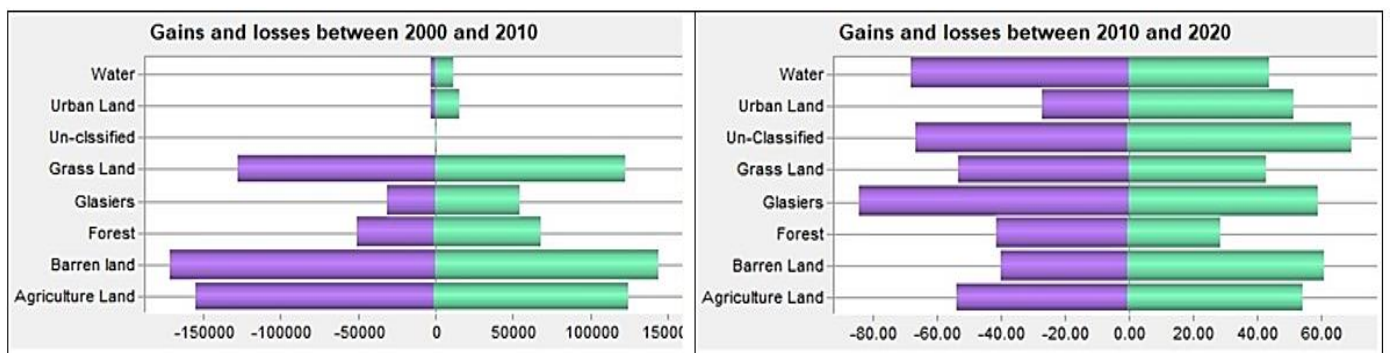


Figure 5. Contribution to Net change of LULC class of the study periods

3.3 Validation of the Model

Using the Validation Module, the two categories' maps' agreement was evaluated. Validation of the Model is required in order to determine correctness. Validation is important since it enables comparing the

projected land cover map's quality with the actual map. In order to verify the anticipated map, a comparison between the real and simulated LULC maps of 2020 was made. Table 6 displays the validation outcomes of the Model between the simulated and actual LULC test summary.

Table 6. Based on the actual and anticipated LULC for 2020, the LULC Change forecast has been validated.

LULC Types	Projected		Actual	
	Km	%	km	%
Urban land	620.51	4.17	541.22	3.67
Agriculture land	2414.87	16.24	2525.08	16.97
Barren land	6029.57	40.54	5530.41	37.18
Forest	1402.57	9.43	1629.62	10.95
Grassland	3877.61	26.07	4247.53	28.55
Water	86.91	0.58	127.94	0.86
Un-classified	80.04	0.54	5.71	0.03
Glaciers	360.61	2.42	265.18	1.78
Total	14872.69	100.00	14872.69	100.00

Table 7 compiles the achieved k-indices. If the Kstandard (overall kappa) value reaches 70%, the Model is considered validated. The predicted and real LULC maps exhibit good agreement, exceeding the minimum acceptable criterion, with values of k-index larger than 80%. Here, all indices are over 80%, demonstrating a solid level of general agreement and the Model's capacity for prediction.

Table 7. The k-index values of the simulated LULC map of 2019.

Index	Value
Kno	0.9026
Klocation	0.9213
KlocationStrata	0.8836
Kstandard	0.874

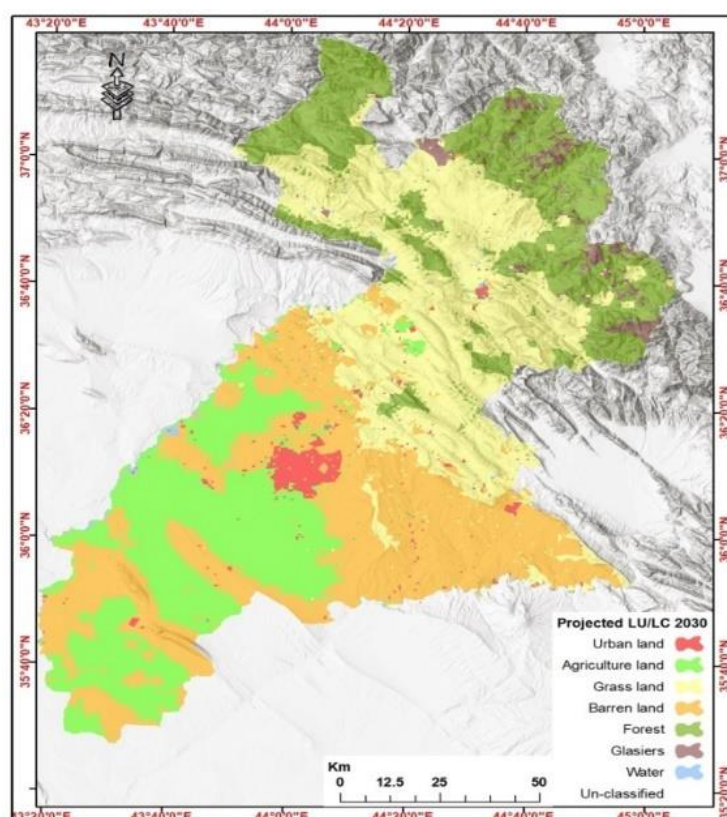
Information on the statistical agreement between the simulated map and the reference map is provided by the values of AgreementQuantity, AgreementChance, Disagreement Grid Cell, AgreementGridCell, and Disagreement Quantity in Table 8. Therefore, to identify the Model's simulated results, Disagreement-GridCell and DisagreementQuantity elements are essential.

Table 8. The k-index values of the simulated LULC map of 2019.

Index	Value	Value Percentage (%)
Agreement Chance	0.1657	16.57
Agreement Quantity	0.2371	23.71
Agreement Gridcell	0.4859	48.59
Disagree Gridcell	0.0762	7.62
Disagree Quantity	0.0351	3.51

In general, there is little difference between the two maps, primarily due to quantity mistakes (0.0351) rather than allocation faults (0.0762). Overall, the simulated and real map have good agreement according to the agreement metrics (99.81 percent). The outcome demonstrates that the Model's capacity to forecast LULC changes in location as opposed to quantity is stronger in the research region. This shows that the Model can model future LULC states and an accurate location definition.

Other researchers claim that the Model was verified by comparing the projected and observed LULC maps for 2020 using the statistics of the kappa index. In many research studies, the kappa coefficient is still a key instrument for measuring accuracy. Because each research region has a unique set of environmental characteristics and circumstances, the LULC change model's effectiveness varies for each study location.

**Figure 6.** The predicted 2030 LULC

3.4 Future LULC Prediction

The year 2030 has been identified as the year of the LULC transition. Therefore, the transition probabilities matrix was used to evaluate the likely future percentages of changes in LULC for the years 2020 through 2030. The two parts of LULC prediction in LCM given by the Markov chain and MLP neural network are the quantity of change and the spatial distribution. Figure 6 displays the simulated future LULC pictures produced from the Model. Similarly, Table 9 provides the area coverage, percentage, and rate of change.

Table 9. The area covered by LULC, the percentage change, and the pace of change in Erbil from 2020 to 2030

LULC Types	Area						Change	
	2000		2010		2020		2020-2030	
	km	%	km	%	km	%	km	%
Urban land	195.00	1.31	296.80	1.45	541.22	3.67	79.29	0.53
Agriculture land	2840.18	19.11	2603.05	17.50	2525.08	16.97	-110.21	-0.74
Barren land	4998.62	23.52	4880.15	21.50	5530.41	37.18	499.16	3.36
Forest	1522.48	20.32	2011.10	22.25	1629.62	10.95	-227.05	-1.53
Grass land	4794.95	32.23	4378.69	31.50	4247.53	28.55	-369.92	-2.49
Water	72.64	0.48	102.73	1.18	127.94	0.86	-41.03	-0.28
Un-classified	5.06	0.03	5.55	0.03	5.71	0.03	74.33	0.50
Glaciers	443.76	2.98	594.62	4.59	265.18	1.78	95.42	0.64

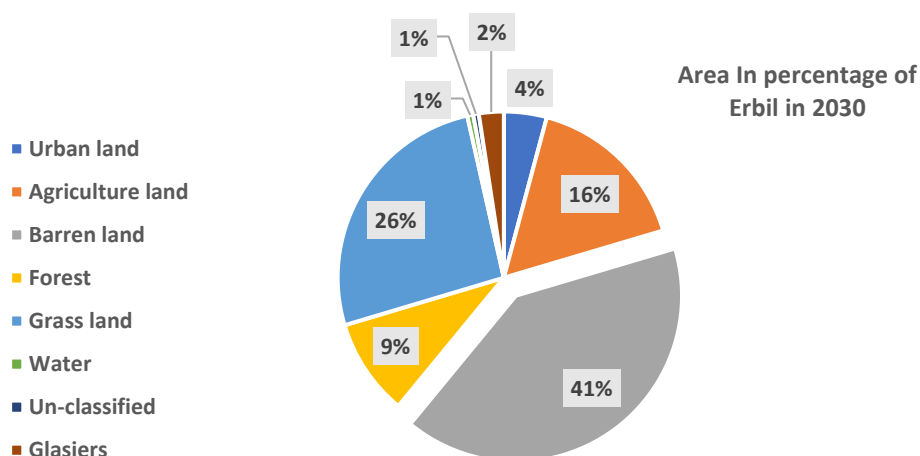


Figure 8. The area coverage of LULC 2030.

According to the change study results, there will be a significant shift in LULC between 1990 and 2050. The majority of LULC will be in the form of agricultural land. The data showed that agricultural land increased from 16.97% in 2020 to 16.24% in 2030. This was mostly brought on by the conversion of agricultural, forestry, and some grassland areas. Between 2000 and 2030, agricultural land decreased dramatically (Figure 8 and Table 9 above). Urban regions and arid terrain had a consistent increase between 2020 and 2030. The urban population will grow due to the construction of infrastructure, industry, and housing that has already occurred and is anticipated to occur in agricultural areas. In 2020, there was 3.67 percent of people living in urban areas; by 2030, that number is expected to rise to 4.17 percent. In Figure 6, the area covered by six LULC classes is graphically shown for the years 2000, 2010, and 2020 as well as for 2030.

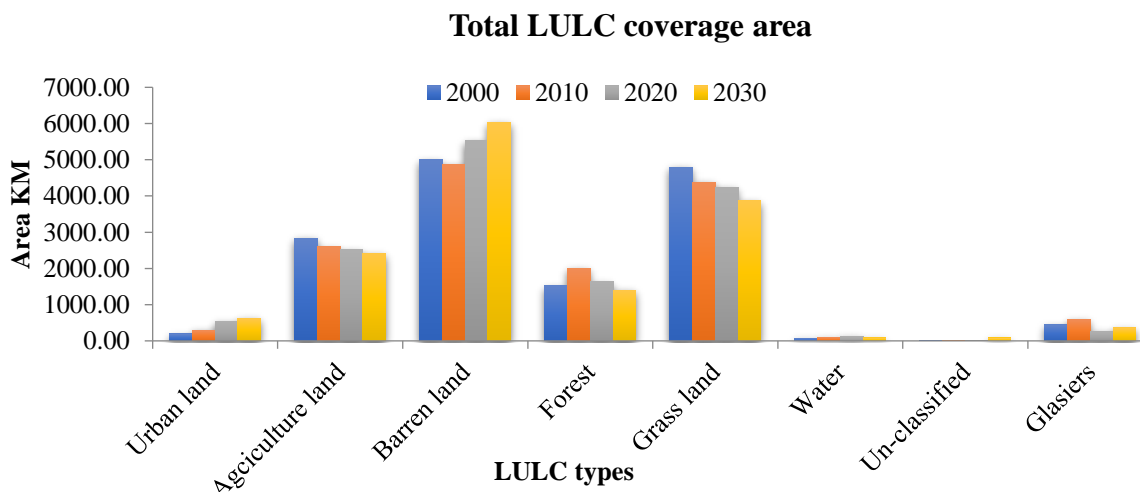


Figure 9. The area coverage of LULC 2000,2010,2020 and 2030.

Between 2020 and 2030, there is a downward tendency in agriculture and forestry. Unfortunately, from 2030, there will be a more built-up and barren land. This might occur due to the restricted amount of land available for various uses. The expanding Urban was one of the main causes of the LULC transformation. Also, we There are some other factors which impact agricultural land, which we assumed from the LULC classification of our Study Area

- More Industrial Activity or high Urbanisation land with less Limitation on it.
- More populous than city capacity has a negative impact on agricultural land.
- Environmental Soil Erosion changes in soil quality or Water consumption are more from its Available quantity.

Most of those residing nearby the forest region, who rely on fuel wood, used charcoal and firewood as their primary energy sources, which contributed to the decrease of the forest. Most people forced to flee during building projects worked on clearing the forest area for development and settlement. Agriculture fields, forest lands, and grasslands were destroyed due to unauthorised and haphazard settlements made by the local population to accommodate growing urban populations. In order to govern and effectively manage agricultural lands and forest conversion, a sensible land use plan needs to be created in an ordered manner. Other LULC classes suffer due to the growth of one LULC type. The government must give the planting and care for trees more attention to the program.

As a result, many devastated places in the nation must grow new covering plants. The area change in the transition matrix was identified in the future prediction of LULC scenarios. According to the study, built-up saw the most growth between the historical data and the forecasts.

Applying management strategies including family planning, soil and water conservation technologies, and encouraging agricultural land use intensification in the research region are important to reduce land degradation. The research area's future land use and land cover change plan must be created in advance and implemented at the policy level.

GIS and remote sensing technologies were used with CA-Markov modeling in LCM-based analysis to analyse the LULC change. The performance of the CA-MC in LCM for the LULC pattern has not yet been assessed in this field of study, as far as the authors know. Additionally, the study region does not undertake assessments of the dynamics of LULC changes and their determinants. As a result, the drivers of LULC dynamics were used to analyse the LULC dynamics of the past and future LULC using Landsat photos and LCM. As a result, this study will also aid in evaluating how well the CA MC strategy performed in the region.

Based on historical LULC change data from 2000-2010, 2010-2020, and 2000-2020, which were utilised as a baseline, a simulation study for 2030 was carried out. The region saw a net loss of agricultural lands, woods, grasslands, and rangelands between 2000 and 2030, consistent with past LULC change analyses. While the developed, arid land and water body gradually increased starting in 2030. Urban land and barren lands are expected to expand from the year 2000 to 2030, according to the projections. To lessen the

long-term negative effects of LULC changes, future land use activities should be based on appropriate land use development and land regulation.

4. Conclusion

The current study aimed to comprehend how historical and projected land use and land cover patterns will evolve between 2000 and 2030. An integrated approach integrating remote sensing, GIS, and a CA-MC model based on MLPNN was deployed in Erbil to explore the spatiotemporal dynamics of LULC and estimate future LULC change. The following conclusions were reached based on the research's findings. First, the multitemporal satellite imaging data support informed decision-making on LULC change by supplying the data needed for tracking and assessing LULC changes. Second, the accuracy of the data from the remotely sensed imagery was evaluated using an error matrix. High-resolution photos from Landsat were employed in the maximum likelihood classification method. A satisfactory result was obtained, and it was handled further for analysis. Third, the anticipated 2020 LULC map and the actual 2020 LULC map were compared to verify the Model. Following successful model validation, the business-as-usual scenario was used to generate the LULC map for 2030. In this process, the LULC data from 2000 to 2010 and 2010 to 2020 served as the baseline and present situation, respectively. Finally, the simulation model's validity was demonstrated by a significant connection between the simulated LULC map and the satellite-derived map.

Modelling urbanisation is a significant technique to forecast the built-up dynamics and comprehend the possible effects of future growth. Although GIS and remote sensing have significant roles, applying the spatial and temporal data is also an important step to help understand how the land use alterations in the earlier periods predict land use in the future, which assists managers, planners, and decision-makers and the planning of sustainable advance policies. For example, this study noticed that the decreasing occurrence of agricultural lands, grassland, and forest areas, at the same time built–areas, and barren lands remarkably increased between 2000 and 2020 (Figure 6).

Analysing the CA-Markov findings yields trustworthy results. The study's findings indicate a fast decline in agricultural, grazing, and forested regions. While. Due to urbanisation, the rapid growth of the population, and the arid landscape, other classes rise over the study time, especially in metropolitan areas.

Studies on LULC changes are extremely helpful for developing nations since they influence the environment because they change so fast.

The Erbil saw big changes in the period 2000-2020 due to socioeconomic and political factors; consequently, the CA-Markov Model offered a true prediction for 2030 because the study area had remarkable changes occurring from 2000 to 2020.

In order to avoid and minimise urbanisation and its effects on agricultural lands, forests, and environmental management, it should also be noted that the study of LULC types provides useful information for decision-making and planners.

Declaration of Competing Interest The authors declare that they have no known competing of interest.

References

- [1] G. Özerol, H. Bressers, and F. Coenen, "Irrigated agriculture and environmental sustainability: an alignment perspective," *Environmental science policy*, vol. 23, pp. 57-67, 2012.
- [2] F. Z. Naab, R. D. Dinye, and R. K. Kasanga, "Urbanisation and its impact on agricultural lands in growing cities in developing countries: a case study of Tamale in Ghana," *Modern Social Science Journal*, vol. 2, no. 2, pp. 256-287, 2013.
- [3] D. H. Ali, "Impact of Factors Immigration from Southern and Capital of Iraq to Erbil City on Local Economic Geographic," *Journal of Studies in Science Engineering*, vol. 1, no. 2, pp. 63-74, 2021.
- [4] X. Deng, J. Huang, S. Rozelle, J. Zhang, and Z. Li, "Impact of urbanization on cultivated land changes in China," *Land use policy*, vol. 45, pp. 1-7, 2015.
- [5] F. Ewert, M. Rounsevell, I. Reginster, M. Metzger, and R. Leemans, "Technology development and climate change as drivers of future agricultural land use," in *Agriculture and climate beyond 2015*: Springer, 2006, pp. 33-51.
- [6] J. Luo, J. Zhan, Y. Lin, and C. Zhao, "An equilibrium analysis of the land use structure in the Yunnan Province, China," *Frontiers of earth science*, pp. 1-12, 2014.
- [7] J. Van Vliet, H. L. de Groot, P. Rietveld, and P. H. Verburg, "Manifestations and underlying drivers of agricultural land use change in Europe," *Landscape Urban Planning*, vol. 133, pp. 24-36, 2015.
- [8] M. W. Holdgate, "The sustainable use of tropical coastal resources-a key conservation issue," *Ambio*, vol. 22, no. 7, pp. 481-482, 1993.
- [9] M. Dadras, H. Z. Mohd Shafri, N. Ahmad, B. Pradhan, and S. Safarpour, "Land use/cover change detection and urban sprawl analysis in Bandar Abbas City, Iran," *The Scientific World Journal*, vol. 2014, 2014.
- [10] A. Singh, "Review article digital change detection techniques using remotely-sensed data," *International journal of remote sensing*, vol. 10, no. 6, pp. 989-1003, 1989.
- [11] D. Langdrige and G. Hagger-Johnson, *Introduction to research methods and data analysis in psychology*. Pearson Education, 2009.
- [12] S. Tajbakhsh, H. Memarian, K. Moradi, A. Aghakhani Afshar, and Management, "Performance comparison of land change modeling techniques for land use projection of arid watersheds," *Global Journal of Environmental Science*, vol. 4, no. 3, pp. 263-280, 2018.